Brain inflammation accompanies amyloid in the majority of mild cognitive impairment cases due to Alzheimer's disease

DOI:
10.1093/brain/awx120

Document Version
Accepted author manuscript

Published in:
Brain

OXFORD UNIVERSITY PRESS | Brain

Brain inflammation accompanies amyloid in a majority of mild cognitive impairment cases due to Alzheimer's disease

Journal:	*Brain*
Manuscript ID	BRAIN-2016-01962.R1
Manuscript Type:	Original Article
Date Submitted by the Author:	05-Mar-2017
Complete List of Authors:	Parbo, Peter; Aarhus University Hospital, Department of Nuclear Medicine and PET Centre Ismail, Rola; Aarhus University Hospital, Department of Nuclear Medicine and PET Centre Hansen, Kim; Aarhus University Hospital, Department of Nuclear Medicine and PET Centre Amidi, Ali; Aarhus University & Aarhus University Hospital, Department of Psychology and Behavioural Sciences & Department of Oncology Mårup, Frederik; Aarhus University Hospital, Department of Nuclear Medicine and PET Centre Gottrup, Hanne; Aarhus University Hospital, Department of Neurology Braendgaard, Hans; Aarhus University Hospital, Department of Neurology Eriksson, Bengt; Hospitalsenheden Midt, Department of Neurology Eskildsen, Simon; Aarhus Universitet, Center of Functionally Integrative Neuroscience Lund, Torben; Aarhus Universitet, Center of Functionally Integrative Neuroscience Tietze, Anna; Aarhus Universitet, Center of Functionally Integrative Neuroscience Edison, Paul; Imperial College London, Neurology Imaging Unit Pavese, Nicola; Aarhus University Hospital, Department of Nuclear Medicine and PET Centre; Imperial College, Division of Brain Sciences Stokholm, Morten; Aarhus University Hospital, Department of Nuclear Medicine and PET Centre Borghammer, Per; Aarhus University Hospital, Department of Nuclear Medicine and PET Centre Hinz, Rainer; University of Manchester Wolfson Molecular Imaging Centre Aanerud, Joel; Aarhus University Hospital, Department of Nuclear Medicine and PET Centre Brooks, David; Aarhus University Hospital, Department of Nuclear Medicine and PET Centre; Imperial College, Division of Brain Sciences
Subject category:	Dementia
To search keyword list, use whole or part words followed by an *:	Mild cognitive impairment < DEMENTIA, Alzheimer's disease < DEMENTIA, Microglia < NEURODEGENERATION: CELLULAR AND MOLECULAR, Amyloid imaging < DEMENTIA, Neuroinflammation < MULTIPLE SCLEROSIS AND NEUROINFLAMMATION

Title:

Brain inflammation accompanies amyloid in a majority of mild cognitive impairment cases due to Alzheimer's disease.

Authors:

Peter Parbo[1], Rola Ismail[1], Kim V. Hansen[1], Ali Amidi[2], Frederik Husum Mårup[1], Hanne Gottrup[3], Hans Brændgaard[3], Bengt O. Erikson[4], Simon F. Eskildsen[5], Torben E. Lund[5], Anna Tietze[6], Paul Edison[7], Nicola Pavese[1,8], Morten Gersel Stokholm[1], Per Borghammer[1], Rainer Hinz[9], Joel A. Aanerud[1], David J. Brooks[1,7,8]

Affiliations:

[1]Department of Nuclear Medicine and PET Centre, Aarhus University Hospital, Aarhus, Denmark

[2]Department of Psychology and Behavioural Sciences & Department of Oncology Aarhus University & Aarhus University Hospital, Denmark

[3]Department of Neurology, Aarhus University Hospital, Aarhus, Denmark

[4]Department of Neurology, Hospitalsenheden Midt, Viborg, Denmark

[5]Center of Functionally Integrative Neuroscience (CFIN), Aarhus University, Aarhus, Denmark

[6]Institute of Neuroradiology, Charité, Universitätsmedizin, Berlin, Germany

[7]Division of Neuroscience, Department of Medicine, Imperial College London, London, UK

[8]Division of Neuroscience, Newcastle University, Newcastle, UK

[9]Wolfson Molecular Imaging Centre, University of Manchester, Manchester, UK

Corresponding author:

Peter Parbo, MD

Department of Nuclear Medicine and PET Centre

Aarhus University Hospital

Nørrebrogade 44, building 10

DK-8000 Aarhus C

Denmark

E-mail: peter.parbo@clin.au.dk

Running title:

Neuroinflammation in mild cognitive impairment

Abstract:

Subjects with mild cognitive impairment (MCI) associated with cortical beta-amyloid have a greatly increased risk of progressing to Alzheimer's disease. We hypothesised that neuroinflammation occurs early in Alzheimer's disease and would be present in most amyloid positive MCI cases. 11C-PiB and 11C-(R)-PK11195 positron emission tomography was used to determine the amyloid load and detect the extent of neuroinflammation (microglial activation) in 42 MCI cases. 12 age-matched healthy controls had 11C-PiB and 10 healthy controls had 11C-(R)-PK11195 positron emission tomography for comparison. Amyloid-positivity was defined as 11C-PiB target-to-cerebellar ratio above 1.5 within a composite cortical volume-of-interest. Supervised cluster analysis was used to generate parametric maps of 11C-(R)-PK11195 binding potential. Levels of 11C-(R)-PK11195 binding potential were measured in a selection of cortical volume-of-interests and at a voxel level. Twenty-six (62%) of 42 MCI cases showed a raised cortical amyloid load compared to healthy controls. Twenty-two (84%) of the 26 amyloid positive MCI cases showed clusters of increased cortical microglial activation accompanying the amyloid. There was a positive correlation between levels of amyloid load and 11C-(R)-PK11195 binding potentials at a voxel level within subregions of frontal, parietal and temporal cortices. 11C-(R)-PK11195 positron emission tomography reveals increased inflammation in a majority of amyloid positive MCI cases, its cortical distribution overlapping that of amyloid deposition.

Keywords:

PK11195; PiB; PET; mild cognitive impairment; Alzheimer; neuroinflammation; beta-amyloid.

Abbreviations:

Aβ = beta-amyloid; BP = binding potential; BPM = biological parametric mapping; CDR = Clinical Dementia Rating; HC = healthy control; GM = grey matter; MBq = megabecquerel; MCI = mild cognitive impairment; MMSE = mini-mental state examination; SPM = statistical parametric mapping; TSPO = Translocator Protein 18kDa; VOI = volume-of-interest.

Introduction

Alzheimer's disease pathology is characterised by abnormal aggregation of the proteins beta-amyloid (Aβ) and hyperphosphorylated tau (Braak and Braak, 1991). The Aβ fibrils form extracellular beta-sheeted plaques, while hyperphosphorylated tau aggregates intracellularly as neurofibrillary tangles (NFTs) composed of insoluble paired helical filaments (PHF) of tau containing both 3- and 4-tubulin site repeats. In the last decade, positron emission tomography (PET) radiotracers have become available to image *in vivo* aggregated Aβ (Klunk *et al.*, 2004) and PHF-tau protein (Xia *et al.*, 2013; Chien *et al.*, 2013). Brain inflammation in the form of microglial activation, its intrinsic immune defence, is also a component of Alzheimer's disease and it has been suggested that it could drive the neurodegenerative processes via cytokine release which promotes tau hyperphosphorylation (Maphis *et al.*, 2015). However, initially microglial activation may play a protective role in prodromal Alzheimer's disease by clearing amyloid, remodelling connections and releasing growth factors (Hamelin *et al.*, 2016). The exact role of the microglial activation in dementias remains uncertain, as does the timing of its response relative to the deposition of Aβ and hyperphosphorylated tau. Activated microglia express translocator protein 18kDa (TSPO) on the outer membrane of their mitochondria. TSPO has an isoquinoline site which binds ^{11}C-(R)-PK11195. Varying extents and levels of microglial activation have been reported using TSPO PET imaging in groups of patients with clinically probable Alzheimer's disease and cases with amnestic mild cognitive impairment (MCI) (Stefaniak and O'Brien, 2015). Recent PET studies have reported both raised and absent baseline TSPO binding in MCI cases (Okello *et al.*, 2009) (Wiley, Brian J. Lopresti, *et al.*, 2009) (Fan *et al.*, 2015) (Hamelin *et al.*, 2016) (Kreisl *et al.*, 2013). When inflammation is present in Alzheimer's disease, it can be seen in areas with high Aβ deposition such as frontal cortex and anterior cingulate, and also in areas with high NFTs density such as medial temporal cortex and hippocampus (Fan *et al.*, 2015).

Subjects with mild cognitive impairment (MCI) have an increased risk of dementia and the amnestic subtype is most likely to progress to Alzheimer's disease (Petersen, 2004). The presence of biomarkers such as hippocampal atrophy on MRI, low $A\beta_{42}$ in cerebrospinal fluid (CSF), and positive Aβ PET increases the likelihood that MCI is caused by Alzheimer's pathology (Albert *et al.*, 2011). Identifying early stages of Alzheimer's disease is of interest, as potential disease-modifying drugs are likely to have the greatest impact, if administered in the early or preclinical stages of the disease. Anti-inflammatory drugs have been suggested as a way of modifying the progression of Alzheimer's disease (Heneka *et al.*, 2015).

In this study, we hypothesised that amnestic MCI cases with PET evidence of cortical Aβ deposition, when compared to MCI cases without raised cortical Aβ and healthy controls, would show cortical microglial activation detectable with ^{11}C-(R)-PK11195 PET.

Materials and methods

Study subjects

MCI subjects were recruited from Dementia/Memory clinics in Jutland and Funen, Denmark, and by newspaper advertisements. Subjects were included if they presented with a history of declining memory function over a minimum of 6 months, preferably corroborated by an informant and in the absence of a history of recreational drug use, sedative medication, depression, stroke or systemic diseases. Further inclusion criteria were: 1) Age 50-85 years; 2) ≥7 years of education or good working history; 3) Meets Petersen criteria (Petersen, 2004) for amnestic MCI (no strict memory score cut-off was used); 4) An informant was available who had frequent contact with the subject and could accompany the subject to clinic visits or be available to talk on the telephone about the subject's memory and complete the interview for Clinical Dementia Rating (CDR); 5) Modified Hachinski Ischemic Scale score ≤ 4; 6) MMSE score 24-30; 7) Geriatric Depression Scale (GDS-15) score ≤ 6; 8) An MRI examination that excluded MCI arising from structural causes.

Exclusion criteria were: 1) Significant neurologic or psychiatric diseases; 2) history of alcohol and/or recreational drug abuse within 2 years; 3) contraindications to MRI; 4) significant reductions in serum B12, red cell folate or thyroid function; 5) use of medication with known anticholinergic effects (which could impair memory) within the last 3 months or a drug that could impair cognition.

Age-matched healthy controls (HC) were recruited by newspaper advertisements and screened for neurological diseases. The same inclusion/exclusion criteria as MCI were applied, except that HC had no complaints of memory decline.

The Central Denmark Region Committees on Health Research Ethics approved the study in accordance with the declaration of Helsinki. All participants signed an informed written consent at enrolment in the study.

Neuropsychological assessment

Neuropsychological assessments were undertaken in all participants with a test battery comprised of different standardized neuropsychological tests assessing multiple cognitive domains. The assessed

cognitive domains and related tests are: 1) *Processing speed:* Coding from Wechsler Adult Intelligence Scale version 4 (WAIS-IV) (Wechsler, 2008), Trail-Making Test Part A (Raitan, 1958) and Stroop Colour and Word Test (Stroop, 1935); 2) *verbal learning and memory:* Rey Auditory Verbal Learning Test (Rey, 1964) and Logical Memory I & II from Wechsler Memory Scale (Wechsler, 1989); 3) *working memory:* Digit span from WAIS-IV (Wechsler, 2008); 4) *visuospatial abilities:* Block design from WAIS-IV (Wechsler, 2008); 5) *language function:* Controlled Oral Word Association Test (Benton, 1989) and the Boston Naming Test (Kaplan *et al.*, 1983); 6) *executive functioning:* Trail-Making Test Part B (Raitan, 1958) and Stroop Colour and Word test (Stroop, 1935). Trained research assistants undertook all assessments under the supervision of an experienced neuropsychology researcher (AA). Normative data were collected from 23 HCs of which 15 were from the present study and eight were included from another study under the same research program. The eight HC did not have PK11195 or PiB PET scans, but they were recruited and had neuropsychological assessments identical to the MCI cohort. One of the 15 controls had a few missing test results, hence N = 22 in some domain and global scores

MRI

Magnetic resonance imaging (MRI) was performed on a Skyra 3 Tesla system (Siemens, Erlangen, Germany). A MP2RAGE (Magnetization Prepared Rapid Gradient-Echo with two gradient echo images) (Marques *et al.*, 2010) sequence was used for co-registration of MRI with PET, normalisation into standard space, and generation of grey matter (GM) masks. MP2RAGE, along with a T2 FLAIR (Fluid Attenuated Inversion Recovery) sequence was used to exclude structural lesions, e.g. tumours and territorial infarction. An experienced neuroradiologist (AT) visually evaluated all the MRIs.

PET

All PET scans were acquired on a High Resolution Research Tomograph (ECAT HRRT; CTI/Siemens, Knoxville, TN, USA). A 6-minute transmission scan was performed prior to each PET emission scan to enable attenuation correction of emission data. Images were reconstructed with a 3D-OSEM (ordered subset expectation maximum) with 10 iterations and 16 subsets. Point-spread function (PSF) reconstruction was applied to minimise partial volume effects, improve image quality, contrast and quantitative accuracy and achieve a reconstructed resolution of 2.5 mm. Images were not partial volume corrected.

Amyloid imaging (PiB PET):

A mean dose of 391 MBq (SD=63) ^{11}C-PiB (Pittsburgh compound B, *N*-methyl-[11C]2-(4-methylaminophenyl)-6-hydroxybenzothiazole) (PiB) was injected intravenously over 10 seconds, followed by a 10 mL saline flush. Subjects rested for 30 minutes after injection before installation in scanner. PET was acquired for 50 minutes in list mode at 40-90 minutes post injection (p.i.). Image data were subsequently re-binned into 5 frames of 10 minutes each.

TSPO imaging (^{11}C-(R)-PK11195 PET):

A mean dose of 390 MBq (SD=47) ^{11}C-(R)-PK11195 (1-[2-chlorophenyl]-N- methyl-N-[1-methyl-propyl]-3-isoquinoline carboxamide) (PK11195) was injected intravenously over 10 seconds, followed by a 10 mL saline flush. Emission scans were initiated with a 30 second "background" frame before injection of PK11195. The total dynamic scan time was 60.5 minutes (list mode). Frames were re-binned as: 1x 30 seconds 'background', 6x 10s, 2x 30s, 2x 60s, 3x 120s, 10x 300s.

Image analysis

MRI volumes were segmented into grey (GM) and white (WM) matter images and CSF using MINC software (http://en.wikibooks.org/wiki/MINC). The GM masks were convolved with a probabilistic atlas (Hammers *et al.*, 2003) to "individualise" subject VOIs to their GM. A weighted average of 5 bilateral regions (inferiolateral parietal, inferior frontal, middle/inferior temporal, posterior cingulate and parahippocampal cortices) were combined to form a composite VOI, used in both PiB and PK11195 analysis. An average GM mask from MCI and healthy subjects was used for explicit masking with Statistical Parametric Mapping 8 (SPM8; Wellcome Trust Centre for Neuroimaging).

^{11}C -PiB RATIO images

PiB images of each individual were co-registered to their T1 MR images, and then the transformation matrices from the individuals T1 space to MNI space were applied to the PET images using MINC tools. The spatially normalised PiB images were summed from 60-90 minutes, and voxel signals divided by the mean signal from the individual's cerebellar GM VOI to generate PiB RATIO images (Edison *et al.*, 2007). Images were not smoothed before extraction of measurements from the composite cortical VOI, to minimise spill-in/spill-out. PiB-positivity was defined from the bimodal MCI distribution as a composite cortical PiB RATIO>1.5. PiB RATIO images were smoothed with a 6 mm full width at half maximum (FWHM) Gaussian filter prior to SPM and BPM analyses.

PK11195 binding potential maps

After smoothing the dynamic PET images with a 4 mm FWHM three-dimensional Gaussian filter, parametric maps of binding potential (BP_{ND}) were generated at a voxel level using the Simplified Reference Tissue Model (SRTM) (Lammertsma and Hume, 1996) implemented in Matlab. As all anatomical regions in the brain can show specific PK11195 binding in Alzheimer's disease, a Supervised Cluster Analysis with 6-classses (Turkheimer *et al.*, 2007) (SVCA6) was used to localise a cluster of voxels from the dynamic images of each MCI case which provided a reference tissue input function representing normal grey matter kinetics. The PK11195 images were spatially normalised into MNI space in the same manner as described for the PiB images. PK11195 images were smoothed with a 6 mm FWHM Gaussian filter prior to SPM and BPM analyses. Levels of PK11195 BP_{ND} are sampled from 13 VOIs, comprising left and right VOIs of 6 cortical regions (frontal, lateral parietal, lateral temporal, medial temporal, precuneus and posterior cingulate) and the composite VOI.

Statistical Parametric Mapping and Biological Parametric Mapping

Clusters of increased PK11195 binding are scattered and so a VOI approach based on Brodmann regions of the brain will include both voxels with raised and normal PK11195 signal. Alongside a *pre-defined* VOI approach, parametric maps of PK11195 BP_{ND} were interrogated with SPM to detect clusters of voxels with significantly increased PK11195 BP_{ND} in the PiB-positive MCI group compared to the HC group. The amplitude of increased microglial activation in these clusters of increased PK11195 BP_{ND} was then quantified, thus avoiding dilution by partial volume effects from surrounding normal voxels – a problem with anatomically based VOIs. SPMs comparing PiB-positive MCI > HC, PiB-positive > PiB-negative MCI, and PiB-negative MCI ≠ HC were generated within a mask defined by the voxels where an ANOVA (uncorrected $p<0.001$) showed a significant mean difference between these three groups (Friston *et al.*, 2006). This map was subsequently thresholded at $p<0.001$ to identify the cluster size corresponding to an FWE corrected cluster level p-value<0.05. This cluster extent was then used as a threshold to construct the final SPMs.

Biological Parametric Mapping (Casanova *et al.*, 2007) (BPM toolbox running in SPM5) was used to detect voxels where there was a positive correlation between individual z-scores of PiB RATIO and PK11195 BP_{ND} in PiB-positive MCI cases. The z-score maps were generated for each PiB-positive MCI case using mean and standard deviation (SD) values from PiB RATIO and PK11195 BP_{ND} maps of healthy controls (PiB n=10 HC, PK11195 n=10 HC).

Statistical analysis

Data were analysed using STATA version 13.1 (StataCorp LP, Texas, USA) and SPSS22 (SPSS Inc., Chicago, Illinois). Differences in non-imaging variables between groups were assessed using ANOVA with post-hoc pairwise mean comparisons (Bonferroni corrected) for normally distributed continuous data, Pearson's χ^2 tests for categorical variables, and Kruskal-Wallis with post-hoc Wilcoxon rank-sum tests (Bonferroni corrected) for skewed ordinal variables. P-values < 0.05 were considered statistically significant. Levels of PK11195 BP were analyzed using a repeated measures two-way ANOVA model with 3 groups (PiB-positive MCI, PIB-negative MCI, control group) and 13 VOIs as inner subject factors. For the neuropsychological data specific z-scores were calculated using test scores from the healthy control group. Domain-specific z-scores were then calculated as the mean of all domain-relevant tests. Between-group differences in the domain-specific z-scores were tested using age-adjusted ANCOVA.

Results

The MCI cohort comprised 42 subjects (mean age 70 years; range 50-83) who had both PiB and PK11195 PET. Fifteen healthy controls (HC) were included in this PET study (mean age 68 years; range 58-80 years), of which 12 HC had PiB PET and 10 HC had PK11195 PET. Seven of the 15 HC had both PiB and PK11195 PET, while the rest had either PiB or PK11195 PET only (see table 1 for further details). The majority of the MCI subjects had their PiB and PK11195 PET scans acquired on the same day. In some cases a tracer production failed and had to be rescheduled. The interval between PIB and PK11195 PET was less than 5 weeks within those MCIs having to return for a rescheduled PET scan. In MCI and controls, the intervals between PET and MRI, and PET and neuropsychological testing were less than 10 and 8 weeks, respectively, with a single control outlier having more than 10 weeks between assessments.

Twenty-six (62%) of the 42 MCI cases had a composite cortical PiB RATIO>1.5 and were categorised as PiB-positive. Two (17%) of the 12 controls were also PiB-positive (Fig. 1) and so represented outliers.

The estimated means of PK11195 BP_{ND} for VOIs are shown in figure 2 with respective 95% confidence intervals. Repeated measures ANOVA revealed a significant group effect ($F(2,49)=7.22$, P=0.0018), whereas regional PK11195 binding did not differ between groups as indicated by non-significant interaction term. Post-hoc group comparisons showed elevated PK11195 binding in the PIB-positive group versus controls (P=0.02) and PIB-negative subjects

(P<0.001). PIB-negative subjects had no difference of PK11195 binding compared to HC (P=0.4). Adjusting for age differences did not change the results.

To estimate the amplitude of focal PK11195 BP_{ND} rises in PiB-positive MCI cases, we measured the PK11195 BP_{ND} within the clusters of voxels of raised BP_{ND} (in total 3652 voxels) localised by statistical parametric mapping (SPM) when interrogating the 26 PiB-positive MCI cases versus 10 HC. SPM identified clusters of significantly raised PK11195 BP_{ND} in PiB-positive MCI individuals targeting the lateral temporal and, to a lesser extent, frontal and parietal areas (Fig. 3A and 3B). PiB-positive MCIs showed a mean PK11195 BP_{ND} of 0.15 (range [0.026–0.39]) within the identified clusters, while controls had a mean of -0.029 (range [-0.088–0.069]). Twenty-two (84%) of the PiB-positive MCI cases had PK11195 binding above the range of controls whereas only 4 (25%) of the PiB-negative MCI had raised PK11195 binding within the same voxels and this was borderline (see Fig. 4). Excluding the two PiB-positive controls from the SPM analysis did not significantly change our findings. HC did not show any clusters with higher PK11195 binding when running the opposite SPM analysis, PiB-positive < HC. An additional small cluster of raised ^{11}C-PK11195 binding was detected in the left hippocampus when PIB-positive MCI were compared with PIB-negative MCI cases, but not when PIB-positive MCI were compared with HC (Fig. 3D and 3E).

Because of differences in mean age between the PiB-positive and PiB–negative MCI group, ANCOVA was performed to extract the variance in PK11195 BP_{ND} at a voxel level arising due to these factors. The age corrected SPMs and uncorrected SPMs showed similar distributions of voxels with significantly raised PK11195 BP_{ND} for the PiB-positive MCI cases.

BPM was used to localise voxels where individual levels of PiB RATIO and PK11195 BP_{ND} had a positive correlation in the group of 26 PiB-positive MCI cases. This approach detected clusters of positive correlation in subregions of frontal, temporal and parietal cortices (Fig. 5A), which differed from the areas of raised PK11195 binding identified in PiB-positive MCI with SPM (Fig. 3A and 3B).

Discussion

This report provides evidence that neuroinflammation is a component of the neurodegenerative pathology present in a majority of Aβ positive MCI; these are the cases who are most likely to progress to Alzheimer's dementia. We detected clusters of raised microglial activation in two-thirds of our PiB-positive MCI cases compared to controls. However, other studies have failed to detect

evidence of microglial activation in MCI (Wiley *et al.*, 2009) (Kreisl *et al.*, 2013). While Wiley *et al.* supported the viewpoint that microglia activation is likely to be an early feature in Alzheimer's disease, they concluded that their ^{11}C-(R)-PK11195 PET study lacked the sensitivity to detect it. Our ability to demonstrate a high prevalence of microglial activation in prodromal Alzheimer's disease could reflect the combined use of a high sensitivity HRRT scanner, a more sensitive SVCA6 kinetic modelling approach, and a larger sample size than previous works.

Nine (35%) of our PiB-positive MCI subjects had PK11195 BP_{ND} values still within the upper normal range. It is, therefore, possible to have amyloid deposition without significant neuroinflammation being present and these MCI cases may prove to progress less rapidly in the future than those with both amyloid plaques and microglial activation evident on PET scanning. However, the opposite situation could be that activated microglia may play a protective role in early AD as suggested by Hamelin et al. The baseline scans of our cases will represent different time points of their disease trajectory and, if inflammation declines as MCI progresses – as suggested in a recent review (Calsolaro and Edison, 2016) and by findings from a recent longitudinal study using ^{18}F-DPA714 PET (Hamelin *et al.*, 2016), this could also account for negative findings in some of our cases. We propose to follow our MCI cohort for a minimum of 2 years and re-scan them to determine their trajectory of inflammation.

The PiB-negative MCI cases all had PK11195 BP_{ND} values within the range of controls. It remains unclear whether such cases have neurodegenerative pathology and will progress to dementia on follow-up. PiB-negative MCI cases represent a heterogeneous group and their memory problems can arise from non-Alzheimer pathologies such as frontotemporal dementia or vascular disease or non-degenerative conditions such as stress, depression, or sleep deprivation, though we have tried to exclude these conditions. Interestingly, two of our normal controls were PiB-positive outliers and they showed no evidence of raised microglial activation. This would favour inflammation arising as a secondary event to Aβ aggregation.

BPM localised brain clusters where there was a significant correlation between levels of amyloid and levels of inflammation. These clusters overlapped but differed from those with raised inflammation detected by a between group SPM analysis comparing PiB-positive MCI cases with controls. This is because BPM identifies voxels where inflammation and amyloid levels are correlated as opposed to voxels where there is a mean increase in inflammation due to any cause. The BPM findings link amyloid deposition and inflammation, particularly in posterior brain regions. However, we cannot exclude that other pathologies may be influencing inflammation with a different distribution to amyloid, like e.g. neurofibrillary tau tangles.

The conservative PiB RATIO cut-off at 1.5 was defined from the bimodal distribution of PiB uptake in our MCI cases and chosen to ensure that the prodromal Alzheimer's disease group we identified had a significant level of cortical amyloid. Additionally, the use of a HRRT scanner provides images with higher sensitivity than the conventional PET-CT cameras usually employed for PiB PET. Use of the HRRT may also provide a greater specific cortical signal due to reduced spill-in to cerebellar grey matter, resulting in higher ratios measured within cerebral cortical regions.

The neuropsychological test results indicated that PiB-positive MCI cases performed significantly worse in the memory domain compared with the PiB-negative MCI cases and healthy controls. Moreover, the testing also indicated that the MCI cohort was clinically heterogeneous in terms of affected domains (see table 1B and supplementary figure 1), which could have increased variance in the size and extent of the regional cerebral PK11195 binding.

In summary, this study provides supportive evidence that neuroinflammation is a component of the neurodegenerative pathology in a majority of MCI cases due to Alzheimer's disease. Statistical parametric mapping localised clusters of raised PK11195 binding in 84% of our Aβ positive amnestic MCI (prodromal Alzheimer's disease) subjects. We found raised inflammation in only 25% of the Aβ negative MCI subjects and this was borderline. The distribution of neuroinflammation in Aβ positive MCI mirrored the distribution of the Aβ in the frontal, temporal and parietal cortices. However, the temporal order of these pathologies still needs to be further investigated and will probably require longitudinal PET studies of high-risk normal subjects. Our MCI cohort will be followed for a minimum of 2 years and rescanned to determine whether neuroinflammation declines or increases with progression towards Alzheimer's disease. On occasion raised Aβ can be detected in MCI and normal subjects without evidence of neuroinflammation. Follow-up of such subjects may determine whether they have a more benign syndrome than the MCI subjects who have both Aβ deposition and neuroinflammation present.

Acknowledgements

We thank Anne Sofie Møller Andersen for great administrative support, consultants Petya Hykkelsbjerg and Lene Wermuth for referring subjects with MCI, Arne Møller for help with PET scans, Zhen Fan for assistance getting started with BPM, and Dora Ziedler, Rune Bæksager Nielsen and Leif Østergaard from the MRI group.

Funding

The study was financially supported by a grant from the Danish Council for Independent Research and the Lundbeck Foundation.

References

Albert MS, DeKosky ST, Dickson D, Dubois B, Feldman HH, Fox NC, et al. The diagnosis of mild cognitive impairment due to Alzheimer's disease: Recommendations from the National Institute on Aging-Alzheimer's Association workgroups on diagnostic guidelines for Alzheimer's disease. Alzheimer's Dement. 2011; 7: 270–279.

Benton A. Multilingual Aphasia Examination. Iowa City: AJA Associates; 1989.

Braak H, Braak E. Neuropathological stageing of Alzheimer-related changes. Acta Neuropathol 1991; 82: 239–259.

Calsolaro V, Edison P. Neuroinflammation in Alzheimer's disease: Current evidence and future directions. Alzheimers Dement. 2016; 12: 719–732.

Casanova R, Srikanth R, Baer A, Laurienti PJ, Burdette JH, Hayasaka S, et al. Biological parametric mapping: A statistical toolbox for multimodality brain image analysis. Neuroimage 2007; 34: 137–143.

Chien DT, Bahri S, Szardenings AK, Walsh JC, Mu F, Su MY, et al. Early Clinical PET Imaging Results with the Novel PHF-Tau Radioligand [F-18]-T807. J. Alzheimer's Dis. 2013; 34: 457–468.

Edison P, Archer H, Hinz R, Hammers A, Tai Y, Hotton G, et al. Amyloid, hypometabolism, and cognition in Alzheimer disease. An [11C]PIB and [18F]FDG PET study. Neurology 2007; 68: 501–508.

Fan Z, Aman Y, Ahmed I, Chetelat G, Landeau B, Ray Chaudhuri K, et al. Influence of microglial activation on neuronal function in Alzheimer's and Parkinson's disease dementia. Alzheimer's Dement. 2015; 11: 608–621.

Friston KJ, Rotshtein P, Geng JJ, Sterzer P, Henson RN. A critique of functional localisers. Neuroimage 2006; 30: 1077–1087.

Hamelin L, Lagarde J, Dorothé G, Leroy C, Labit M, Comley RA, et al. Early and protective microglial activation in Alzheimer's disease: a prospective study using 18 F-DPA-714 PET imaging. Brain 2016: 1252–1264.

Hammers A, Allom R, Koepp MJ, Free SL, Myers R, Lemieux L, et al. Three-dimensional maximum probability atlas of the human brain, with particular reference to the temporal lobe. Hum. Brain Mapp. 2003; 19: 224–247.

Heneka MT, Carson MJ, Khoury J El, Landreth GE, Brosseron F, Feinstein DL, et al. Neuroinflammation in Alzheimer's disease. Lancet Neurol. 2015; 14: 388–405.

Kaplan E, Goodglass H, Weintraub S. The Boston Naming Test. Philadelphia: Lea & Febiger; 1983.

Klunk W, Engler H, Nordberg A, Wang Y, Blomqvist G, Holt DP, et al. Imaging Brain Amyloid in Alzheimer's Disease with Pittsburgh Compound-B. Ann. Neurol. 2004; 55: 306–319.

Lammertsma AA, Hume SP. Simplified reference tissue model for PET receptor studies. Neuroimage 1996; 158: 153–158.

Maphis N, Xu G, Kokiko-Cochran ON, Jiang S, Cardona a., Ransohoff RM, et al. Reactive microglia drive tau pathology and contribute to the spreading of pathological tau in the brain. Brain 2015; 138: 1738-55.

Marques JP, Kober T, Krueger G, van der Zwaag W, Van de Moortele PF, Gruetter R. MP2RAGE, a self bias-field corrected sequence for improved segmentation and T1-mapping at high field. Neuroimage 2010; 49: 1271–1281.

Okello A, Edison P, Archer HA, Turkheimer FE, Kennedy J, Bullock R, *et al*. Microglia activation and amyloid deposition in mild cognitive impairment: a PET study. Neurology 2009; 72: 56-62.

Petersen RC. Mild cognitive impairment as a diagnostic entity. J. Intern. Med. 2004; 256: 183–94.

Raitan R. Validity of the Trail Making test as an indicator of organic brain damage. Percept. Mot. Ski. 1958; 8: 271–276.

Rey A. L'examen Clinique en Psychologie. City, France: Universitaires de France; 1964.

Stefaniak J, O'Brien J. Imaging of neuroinflammation in dementia: a review. J. Neurol. Neurosurg. Psychiatry 2015: 21–28.

Stroop J. Studies of interference in serial verbal reactions. J. Exp. Psychol. 1935; 18: 643–662.

Turkheimer FE, Edison P, Pavese N, Roncaroli F, Anderson AN, Hammers A, et al. Reference and target region modeling of 11C-(R)-PK11195 brain studies. J. Nucl. Med. 2007; 48: 158–167.

Wechsler D. Wechsler Memory Scale. Third Edit. San Antonio, TX: Pearson; 1989.

Wechsler D. Wechsler Adult Intelligence Scale. Fourth Edi. San Antonio, TX: Pearson; 2008.

Wiley CA, Lopresti BJ, Venneti S, Price J, Klunk WE, DeKosky ST, et al. Carbon 11-labeled Pittsburgh Compound B and carbon 11-labeled (R)-PK11195 positron emission tomographic imaging in Alzheimer disease. Arch. Neurol. 2009; 66: 60–7.

Xia CF, Arteaga J, Chen G, Gangadharmath U, Gomez LF, Kasi D, et al. [(18)F]T807, a novel tau positron emission tomography imaging agent for Alzheimer's disease. Alzheimers. Dement. 2013; 9: 666–76.

Table 1A: Participant characterisation.

	PiB+ MCI (N = 26)	PiB- MCI (N = 16)	Healthy controls (N = 15)	P-value
Age (years) Mean ± SD [Range]	73.3 ± 6.2 [62-83]	65.8 ± 8.4 [50-79]	68.3 ± 6.6 [58-80]	0.003[a]
Gender, males N (%)	17 (65%)	7 (44%)	6 (40%)	0.2
Education (years): Median	12	11.5	13	0.2
Number (%) of subjects using NSAID	9 (35%)	4 (25%)	1 (7%)	0.1
MMSE score Median [Range]	27 [23-30]	28 [23-30]	29 [25-30]	0.005[b]
CDR sum of boxes Median	1.5	1	0	0.0001[b, c]
PiB dose (MBq) Mean ± SD (N)	365 ± 79	409 ± 25	422 ± 28 (N = 12)	0.01[b]
PK11195 dose (MBq) Mean ± SD (N)	384 ± 47	375 ± 57	389 ± 21 (N = 10)	0.9
Fazekas score Median (N)	1 (N = 25)	1	0.5 (N = 14)	0.04[b]

Table 1B: Neuropsychological testing.

	PiB+ MCI (N = 26)	PiB- MCI (N = 16)	P-value
Processing Speed Mean z-score ± SD	-1.5 ± 0.8	-0.7 ± 1.1	<0.0001[b, c]
Working memory Mean z-score ± SD	-0.6 ± 1.0	-0.2 ± 1.4	0.4
Visuospatial function Mean z-score ± SD	-0.9 ± 1.9	- 0.2 ± 1.7	0.5
Global memory Mean z-score ± SD	-1.5 ± 1.0	-0.5 ± 1.2	<0.0001[b]
Language Mean z-score ± SD	- 0.9 ± 1.1	-0.8 ± 1.7	0.06
Executive function Mean z-score ± SD	-1.2 ± 0.9	-0.4 ± 1.3	0.004[b]
Global composite score Mean z-score ± SD	-1.2 ± 0.8	-0.4 ± 1.1	<0.0001[b]

Table 1 (A & B): Participant characterisation and neuropsychological testing.

Data are presented as mean ± SD, number of subjects (%) or medians. Differences between groups are tested (using ANOVA, Pearson's χ^2 or Kruskal-Wallis), and resulting P-values are presented in the rightmost column. 1A: One PiB+ MCI and one control subject did not have T2 FLAIR, hence missing Fazekas scores. 1B: Neuropsychological domain and global z-score differences between groups were assessed using age-adjusted ANCOVA across the three groups PiB+ MCI, PiB- MCI and healthy controls (latter not presented in table). 1A & 1B: Post-hoc pairwise group comparisons (Bonferroni corrected), [a] $P < 0.05$ for PiB+ MCI vs PiB- MCI; [b] $P < 0.05$ for PiB+ MCI vs controls; [c] $P < 0.05$ for PiB- MCI vs controls.

MCI=Mild cognitive impairment, PiB+=PiB-positive MCI, PiB-=PiB-negative MCI, SD=standard deviation, MBq=megabecquerel, NSAID=Non-steroidal anti-inflammatory drug, MMSE=Mini-mental state examination, CDR=Clinical dementia rating.

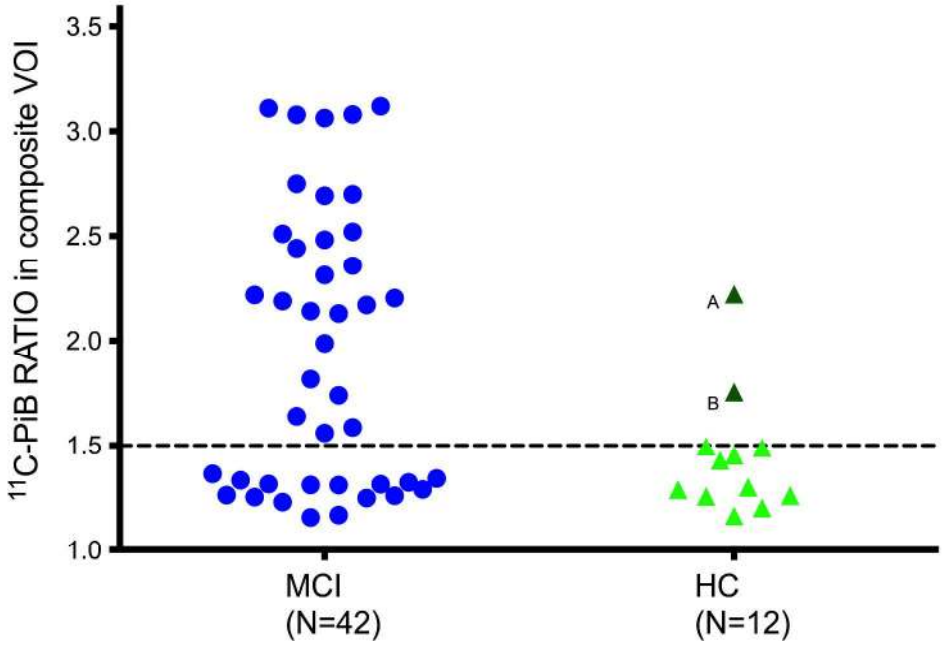

Figure 1: Scatterplot of 11C-PiB RATIO in composite cortical VOI.
Twenty-six (62%) of MCI cases were above the 1.5 cut-off line, and hence classified as PiB-positive MCI.
The two PiB-positive healthy controls (HC) are marked with the letters 'A' and 'B' for identification in figure 4.

272x181mm (300 x 300 DPI)

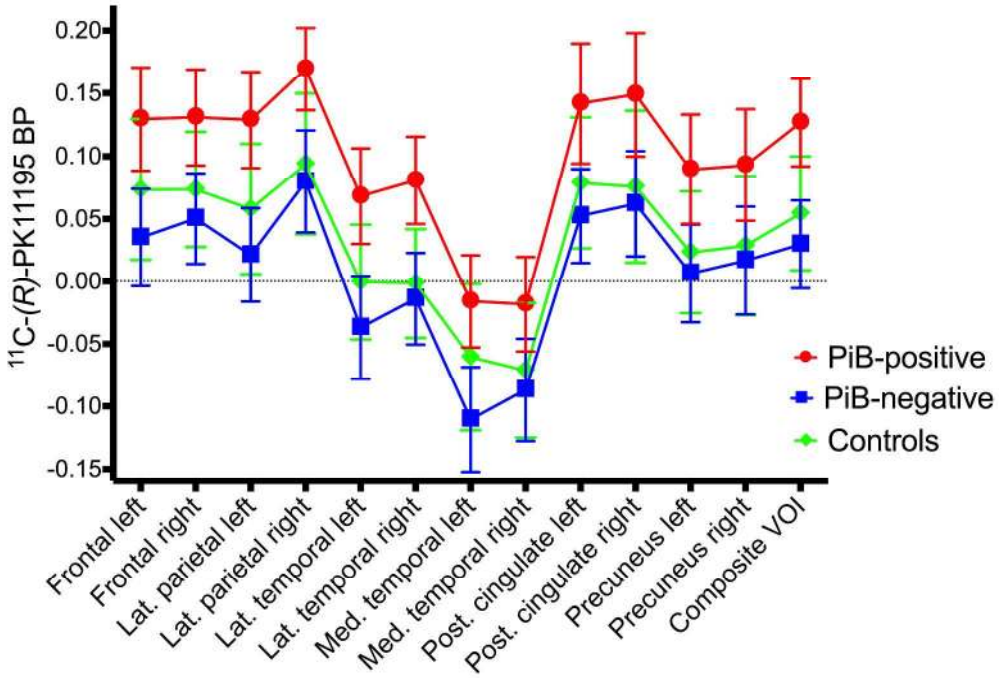

Figure 2: Regional PK11195 BPND in PiB-positive MCI, PiB-negative MCI and healthy controls. Means and 95% confidence intervals of PK11195 BPND in left and right frontal, lateral parietal, lateral and medial temporal, precuneus and posterior cingulate cortical VOIs, and the composite VOI. Repeated measures ANOVA revealed a significant group effect ($F(2,49)=7.22$, $P=0.0018$). Post-hoc group comparisons showed elevated PK11195 binding in the PIB-positive group compared to controls ($P = 0.02$) and PIB-negative subjects ($P < 0.001$).

265x185mm (300 x 300 DPI)

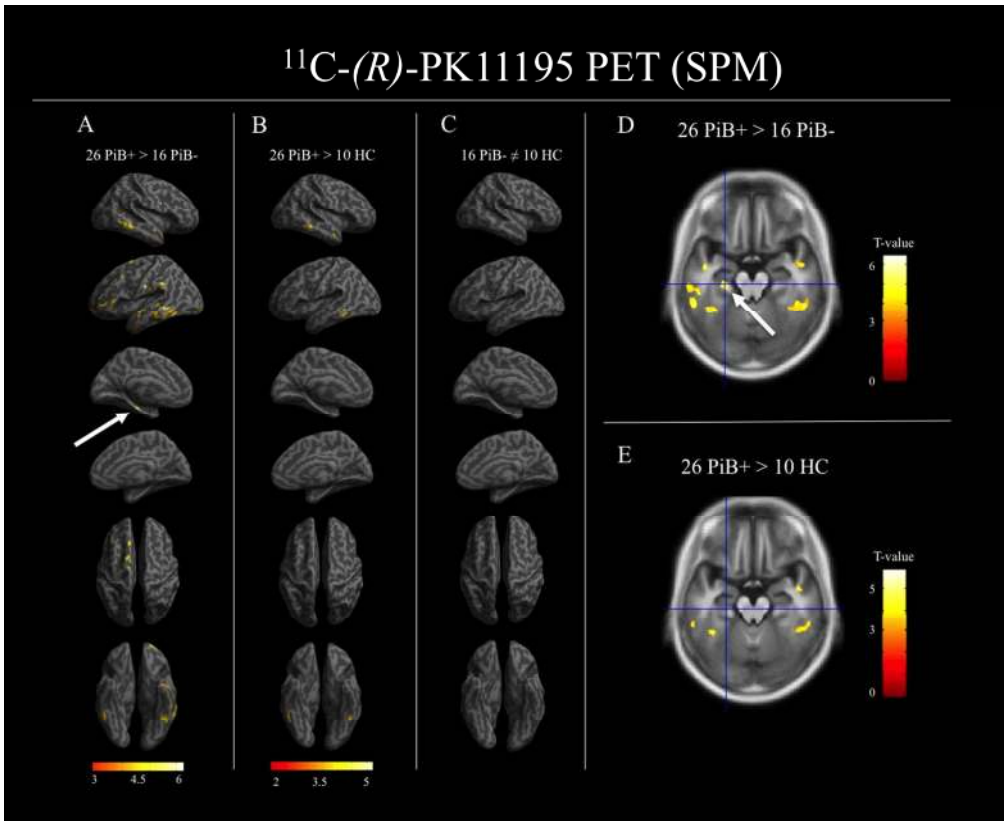

Figure 3: Results from SPM analyses of group comparisons of PK11195 BPND maps.
A-C: Two-sample t-tests between PiB-positive and PiB-negative MCI, PiB-positive MCI and healthy controls (HC), and between PiB-negative MCI and HC. D-E: PiB+ MCI > PiB- MCI reveals a cluster in the left hippocampus (marked with a white arrow in figure 3A and 3D). This hippocampal cluster is not seen in the PiB+ MCI > HC comparison (figure 3E, cross hair positioned in same coordinate as in figure 3D. All comparisons are processed within a mask defined by a voxel-wise ANOVA, and the displayed clusters are of significant size (FWE cluster-level $p<0.05$, with a cluster-defining threshold of $p<0.001$).

423x344mm (72 x 72 DPI)

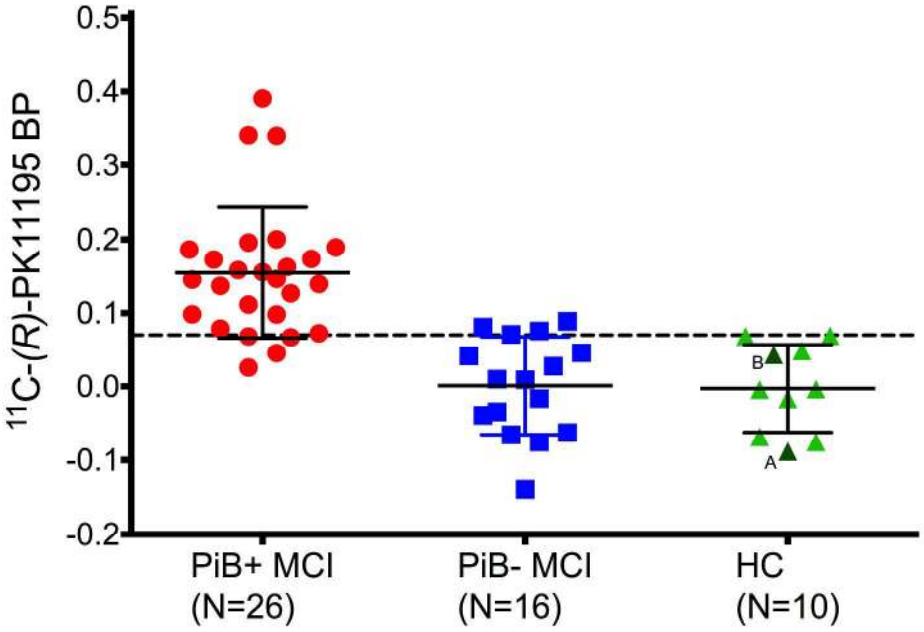

Figure 4: Scatterplot of individual PK11195 BPND across clusters localised by the SPM.
Individual PK11195 BPND levels averaged across all voxels contained in the clusters localised by the SPM comparing PiB-positive MCI with HCs (Fig. 3-B). Twenty-two (84%) of the 26 PiB-positive MCI cases showed PK11195 binding levels above the HC range. PK11195 BPND levels for individual PiB-negative MCI and HC subjects averaged across voxels at the same locations are also shown in the plot. Letters 'A' and 'B' indicates the two PiB-positive controls seen in figure 1. The dashed horizontal line at y=0.07 marks the upper limit of the HC range; short solid lines are group means; dotted lines indicate ±1SD.

271x176mm (300 x 300 DPI)

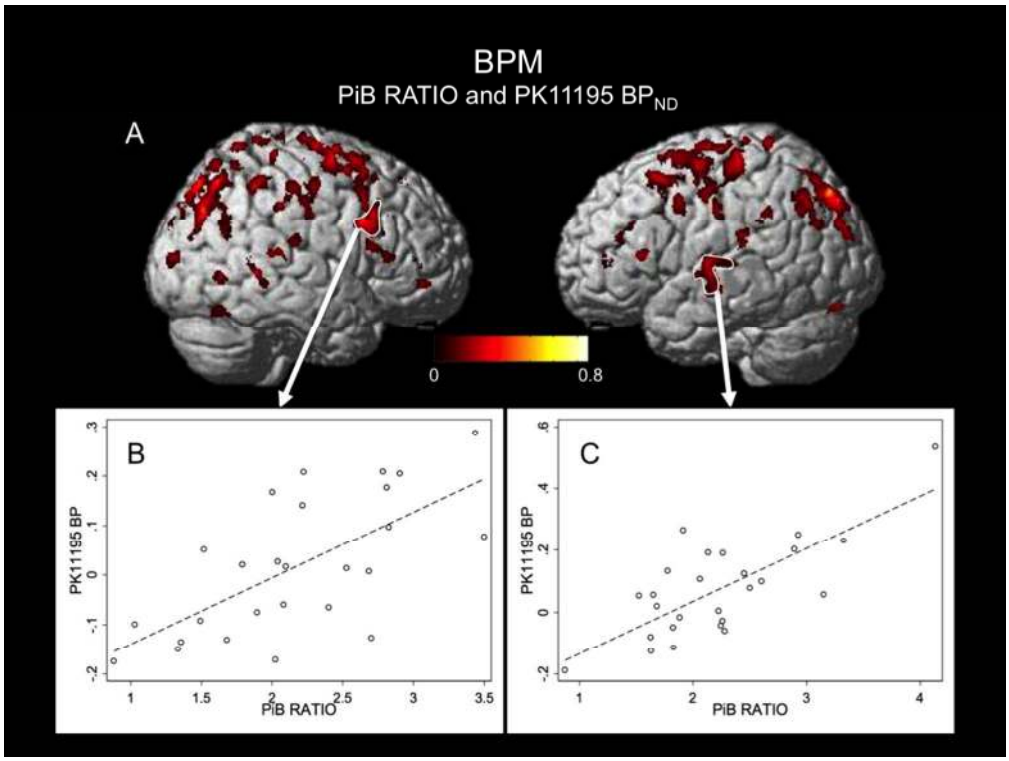

Figure 5: Biological Parametric Mapping (BPM) of PiB RATIO and PK11195 BPND.
A: Clusters of voxels with a positive correlation between PiB RATIO and PK11195 BPND within 26 PiB-positive MCI cases. Voxel-level uncorrected P < 0.001, cluster-level corrected at P < 0.05. B and C: Two clusters are picked for extraction of individual measures of the 26 PiB-positive MCI cases (B, right inferior frontal gyrus; C, left superior temporal gyrus).

423x317mm (72 x 72 DPI)

Supplementary table 1: Drug use and time delay between assessments.

	PiB+ MCI (N = 26)	PiB- MCI (N = 16)	Healthy controls (N = 15)
Anti-hypertensive drug use	12 (46%)	8 (50%)	1 (7%)
Anti-diabetic drug use	2 (8%)	0 (0%)	0 (0%)
Anti-cholesterol drug use	7 (27%)	1 (6%)	3 (20%)
Number of days between:			
PK11195 and PiB PET	4.8 ± 11.4	5.8 ± 10.9	34.7 ± 33.0 (N=7)
PK11195 PET and MR	25.9 ± 17.4	17.3 ± 17.2	43.3 ± 59.1 (N=10)
PK11195 PET and neuropsychological testing	20.3 ± 16.4	13.1 ± 11.4	34.8 ± 52.2 (N=10)
PiB PET and MRI	21.6 ± 16.2	14.6 ± 11.8	44.0 ± 34.3 (N=12)
PiB PET and neuropsychological testing	17.0 ± 15.9	13.0 ± 10.2	36.3 ± 40.0 (N=12)
MRI and neuropsychological testing	8.2 ± 13.9	5.7 ± 11.3	12.1 ± 15.8 (N=15)

Supplementary table 1: Drug use and number of days between different assessments.

The interval between PIB and PK11195 PET was less than 5 weeks within the MCI groups. In MCI and controls, the intervals between PET and MRI, and PET and neuropsychological testing were less than 10 and 8 weeks, respectively, with two controls being outliers having more than 10 weeks between assessments. Data are presented as number of subjects (%) or mean ± SD. MCI=Mild cognitive impairment, PiB+=PiB-positive MCI, PiB-=PiB-negative MCI, PET=Positron emission tomography, MRI=Magnetic resonance imaging.

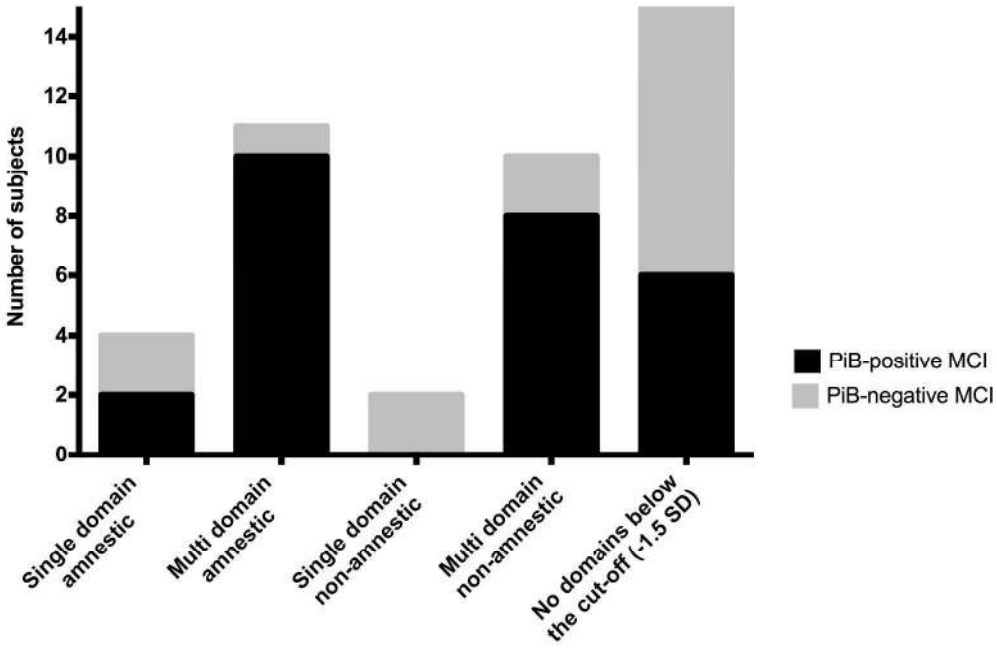

272x181mm (300 x 300 DPI)